ELSEVIER

Biophysical Chemistry 59 (1996) 75–86

Biophysical Chemistry

Regulation of cytochrome oxidase: theoretical studies

Bernard Korzeniewski [1]

Institute of Molecular Biology, Jagiellonian University, al. Mickiewicza 3, 31-120 Kraków, Poland

Received 28 January 1995; revised 14 August 1995; accepted 22 September 1995

Abstract

Using the dynamic model of oxidative phosphorylation developed previously and tested for its validity under a broad range of conditions some properties of cytochrome oxidase in the whole system considered were simulated. The regulation of this enzyme by oxygen concentration, Δp and reduction level of cytochrome c were studied. Assuming at least qualitative validity of the model, the following conclusions were drawn: (1) Regulation of cytochrome oxidase is different under the same conditions, when changes in the system (oxidative phosphorylation in isolated mitochondria) are imposed by a decrease in oxygen concentration (aerobiosis → anaerobiosis transition) or by addition of hexokinase (state 4 → state 3 transition). In the former case, cytochrome c and Δp play a very similar role in the compensation for a decrease in the respiration rate caused by lowered oxygen concentration, while in the latter case changes in Δp activate cytochrome oxidase much stronger than changes in the reduction level of cytochrome c. (2) There is no unique thermodynamic flux–force relationship for cytochrome oxidase. This relationship depends on how the thermodynamic span of the reaction catalyzed by this enzyme is changed (aerobiosis → anaerobiosis transition vs. state 4 → state 3 transition). (3) Under some conditions (aerobiosis → anaerobiosis transition) the flux–force relationship can be inverse, i.e. increase in a thermodynamic force occurs simultaneously with decrease in a reaction rate.

Keywords: Cytochrome oxidase; Kinetics; Thermodynamics; Oxidative phosphorylation; Dynamic model

1. Introduction

Cytochrome oxidase is the terminal component of the respiratory chain, catalyzing transfer of electrons from cytochrome c to oxygen. This transfer is coupled with proton pumping outside the mitochondria, equivalent to building up the proton-motive force (Δp). The reaction catalyzed by cytochrome oxidase is far from thermodynamic equilibrium and essentially irreversible. Therefore it is not necessarily expected to exhibit a simple linear dependence on the thermodynamic span, characteristic for reactions being near equilibrium. Nevertheless, it is commonly (although implicitly) accepted that this dependence for a given system or reaction is unique under the same conditions and proportional (flux increases when force increases) [1–3].

On the other hand, negative values of the thermodynamic response coefficient for cytochrome oxidase at lower (but still physiological) oxygen concentra-

[1] Tel.: (48-12) 342008; Fax: (48-12) 336907; e-mail: benio@mol.uj.edu.pl.

SSDI 0301-4622(95)00121-2

tions were calculated for the case when oxygen was gradually consumed by cells suspended in a closed chamber and thus oxygen concentration decreased to zero [4]. The thermodynamic response coefficient describes the relative change in the thermodynamic span of a given reaction as compared to the change in the thermodynamic span through the entire considered system. This coefficient was defined as follows [4]:

$$T_{ijk} = \delta\Delta G_i / \delta\Delta G_j r_{ij} \quad (1)$$

where k, j and i denote the indices of the external metabolite (substrate or product), M_k, whose concentration is changed, of the considered system U_j and of an enzyme e_i (being a component of this system), respectively. $\delta\Delta G_i$ and $\delta\Delta G_j$ stand for the infinitesimal changes in the Gibbs free energy difference of the reaction catalyzed by enzyme e_i, and in the Gibbs free energy difference of the whole considered system U_j, respectively. r_{ij} denotes the relative flux through the enzyme e_i. The negative value of the thermodynamic response coefficient for cytochrome oxidase during transition to anaerobiosis means that the thermodynamic span of the reaction catalyzed by this enzyme increases when ΔG of the whole oxidative phosphorylation system (and the flux through this system) decreases. This suggests the possibility that the flux–force relationship for this enzyme could be inverse, not proportional. Values of the thermodynamic response coefficient for different components of oxidative phosphorylation depended on the way in which the thermodynamic span through the whole system was changed [4]. This indicates that the flux–force relationship could not be unique. In the present paper these problems are studied more thoroughly and explicitly, applying an improved and tested in much more aspects version of the model.

Cytochrome oxidase, working far from equilibrium, is likely to be regulated kinetically and not thermodynamically [5]. The factors affecting the reaction rate of this enzyme in mammalian cells are oxygen concentration, reduction level of cytochrome c and Δp [6–8]. The previous opinions concerning regulation of cytochrome oxidase by the external [ATP]/[ADP][P_i] ratio [6,9] have been not confirmed. Oxygen is an external substrate for oxidative phosphorylation. Therefore, although the cell has to respond to changes in its concentration, it is not a regulatory factor. Thus, two "regulators" remain: cytochrome c and Δp. A question arises as to their quantitative significance under physiological (or quasi-physiological) conditions. Another problem concerns possible differences in their relative "regulatory power" when different changes are introduced to the system under the same conditions. Two kinds of such changes have physiological significance. The first kind is the varying energy demand, which can be mimicked in isolated mitochondria by addition of increasing amounts of hexokinase (in the presence of glucose) to mitochondria in state 4 (state 4 → state 3 transition). The other change occurring in intact tissues is decrease in oxygen concentration, or even its (almost) total exhaustion, which takes place, for example, in skeletal muscle during prolonged exercise. This case can be studied in suspensions of cells or mitochondria with decreasing values of fixed oxygen concentration (aerobiosis → anaerobiosis transition).

2. Model

2.1. Rate expressions

The dynamic model of oxidative phosphorylation used in this paper was developed in several steps and published in subsequent papers [10–13]. For this reason, the final description of the model has not been published anywhere in one piece. Therefore, I will give below a concise description of the final version of the model. Those details will be pointed out which are different in the version for intact cells (hepatocytes) and the version for isolated rat liver mitochondria incubated with succinate. The numbers of equations concerning exclusively mitochondria will be signed with an asterisk (*).

The expressions for the reaction rates of particular steps of oxidative phosphorylation taken into account explicitly are presented below. The values of rate constants are not given as they are not fixed, but calculated in the initial state (see below) on the basis of fixed parameter values (for example Michaelis–Menten constants) as well as initial values of concentrations and fluxes.

2.1.1. Substrate dehydrogenation

$$v_{DH} = k_{DH} \frac{1}{\left(1 + \frac{K_{mN}}{[NAD^+]/[NADH]}\right)^{p_D}} \quad (2)$$

$K_{mN} = 100$ is the Michaelis–Menten constant for the $NAD^+/NADH$ ratio and $p_D = 0.18$ is a phenomenological parameter reflecting the sensitivity of substrate dehydrogenation to this ratio. In the version of the model concerning isolated mitochondria respiring on succinate another rate expression was used:

$$v_{DH} = k_{DH}([U]_0 - [UQH_2]) \quad (2^*)$$

where $[U]_0 = 0.7[U]_t$ is a phenomenological constant and $[U]_t = [UQ] + [UQH_2]$ denotes total concentration of ubiquinon.

2.1.2. Cytochrome oxidase

$$v_{c4} = k_{c4}[a^{2+}][c^{2+}] \frac{1}{1 + \frac{K_{mO}}{O_2}} \quad (3)$$

$K_{mO} = 12$ μM is the "real" Michaelis–Menten constant for oxygen (the apparent constant is much smaller, equal to about 1 μM, because of regulation of cytochrome oxidase by Δp and cytochrome *c*), while a^{2+} and c^{2+} denote reduced forms of cytochromes a_3 and c, respectively.

2.1.3. ATP synthase

$$v_{SN} = k_{SN} \frac{\gamma - 1}{\gamma + 1} \quad (4)$$

$\gamma = 10^{\Delta G_{SN} F/Z}$ denotes the displacement from equilibrium of the reaction catalyzed by ATP synthase and $\Delta G_{SN} = n_A \Delta p - \Delta G_P$ is the Gibbs free energy difference for this reaction (n_A, H^+/ATP stoichiometry, ΔG_P, internal phosphorylation potential).

2.1.4. ATP / ADP carrier

$$v_{EX} = k_{EX}\left(\frac{[ADP_{fe}]}{[ADP_{fe}] + [ATP_{fe}]10^{-\Psi_e/Z}} - \frac{[ADP_{fi}]}{[ADP_{fi}] + [ATP_{fi}]10^{-\Psi_i/Z}}\right) 10^{\Delta G_{EX}/Z p_E} \quad (5)$$

$p_E = 0.3$ is a phenomenological coefficient and

$$\Delta G_{EX} = \Delta\Psi F - RT \ln\left(\frac{[ATP_{fe}][ADP_{fi}]}{[ADP_{fe}][ATP_{fi}]}\right)$$

is the thermodynamic span of the reaction. $\Psi_i = 0.65 \cdot \Delta\Psi$ and $\Psi_e = -0.35 \cdot \Delta\Psi$ represent the "effective fractions" of membrane potential, driving the electrogenic transport of ATP (for exchange with ADP) from inside and from outside the mitochondria, respectively.

2.1.5. Phosphate carrier

$$v_{PI} = k_{P_i}\left([P_{i_e}][H_e] - [P_{i_i}][H_i]\right) \quad (6)$$

2.1.6. ATP usage

$$v_{UT} = k_{UT} \frac{1}{1 + \frac{K_{mA}}{[ATP_{te}]}} \quad (7)$$

K_{mA} is the Michaelis–Menten constant for ATP. The value of this constant is equal to 300 μM in cells and 150 μM for hexokinase in the model for mitochondria.

2.1.7. Proton leak

$$v_{LK} = k_{LK1}(10^{k_{LK2}\Delta\Psi} - 1) + k_{LK3}\Delta p \quad (8)$$

where $k_{L1} = 9.2 \times 10^{-7}$ μM H^+ s^{-1}, $k_{L2} = 9.4 \times 10^{-2}$ mV^{-1} and $k_{L3} = 1.5 \times 10^{-2}$ μM H^+ mV^{-1} s^{-1}.

2.1.8. Adenylate kinase

$$v_{AK} = k_{AKf}[ADP_{fe}][ADP_{me}] - k_{AKb}[ATP_{me}][AMP_e] \quad (9)$$

2.2. Set of differential equations

The rates of changes in time of independent variables were expressed as a set of differential equations. This set is given below:

$$d[NADH]/dt = (v_{DH} - 2v_{c4})/b_N \quad (10a)$$

$$d[UQH_2]/dt = (v_{DH} - 2v_{c4}) \quad (10a^*)$$

$$d[H_i^+]/dt = (n_c v_{c4} - n_A v_{SN} - u v_{EX} - (1-u) v_{PI} - v_{LK}) R_{cm} R_{sc} / b_H \quad (10b)$$

$$d[ATP_{ti}]/dt = (v_{SN} - v_{EX}) R_{cm} R_{sc} \quad (10c)$$

$$dP_{i_{ti}}/dt = (v_{PI} - v_{SN}) R_{cm} R_{sc} \quad (10d)$$

$$d[ATP_{te}]/dt = (v_{EX} - v_{UT} + v_{AK}) R_{sc} \quad (10e)$$

$$d[ATP_{te}]/dt = (v_{EX} - v_{UT} + v_{AK}) \quad (10e^*)$$

$$d[ADP_{te}]/dt = (v_{UT} - v_{EX} - 2v_{AK}) R_{sc} \quad (10f)$$

$$d[ADP_{te}]/dt = (v_{UT} - v_{EX} - 2v_{AK}) \quad (10f^*)$$

$$dP_{i_{te}}/dt = (v_{UT} - v_{PI}) R_{sc} \quad (10g)$$

$$dP_{i_{te}}/dt = (v_{UT} - v_{PI}) \quad (10g^*)$$

R_{cm} and R_{sc} are ratios of cell volume to mitochondrial volume and of suspension volume to cell volume, respectively. $b_N = 5$ denotes the buffering coefficient of the [NADH]/[NAD$^+$] ratio by the β-hydroxybutyrate/acetoacetate ratio [10], while b_H (calculated) stands for buffering coefficient for internal protons [10]. n_A denotes the [H$^+$]/[ATP] stoichiometry, n_c is the number of protons pumped by the respiratory chain per four passing electrons (20 in intact cells and 12 in mitochondria respiring on succinate) and u is equal to $\Delta\Psi/\Delta p$. Since oxygen concentration was fixed in all simulations, the differential equation for oxygen is omitted.

Time-dependent changes of independent variable values were simulated by solving numerically the above set of differential equations using the Gear procedure. Programs were written in Microsoft FORTRAN. An IBM PC/386 compatible computer was used for simulations.

2.3. Parameters and dependent variables

The values of dependent variables were calculated at each iteration step from the values of fixed (or calculated) parameters and independent variables, calculated directly by the Gear procedure.

Concentration of NAD$^+$ was calculated from overall concentration of NAD ($n_t = [NAD^+] + [NADH]$), equal to 8.8 μM (determined in suspension for 3 mg of mitochondrial protein per ml), and from concentration of NADH:

$$[NAD^+] = n_t - [NADH] \quad (11)$$

Concentration of UQ in the version of the model concerning mitochondria was obtained similarly.

Concentrations of ADP_{ti} and AMP_e were calculated in an analogous way:

$$[ADP_{ti}] = A_i - [ATP_{ti}] \quad (12)$$

$$[AMP_e] = A_e - [ATP_{te}] - [ADP_{te}] \quad (13)$$

where $A_i = [ATP_{ti}] + [ADP_{ti}]$ and $A_e = [ATP_{te}] + [ADP_{te}] + [AMP_e]$.

Concentration of external protons was calculated under the assumption that the external buffering capacity for protons was 10 times greater than the internal capacity:

$$[H_e^+] = ([H_t] - [H_i^+])/10 \quad (14)$$

where $[H_t] = ([H_i^+] + [H_e^+])/10$ denotes the sum of free internal and external proton concentrations. Concentration of external protons changes relatively very slightly and, in fact, can be considered as essentially constant, without any significant effect on results of simulations.

The (components of the) proton-motive force were calculated as follows:

$$\Delta pH = \frac{RT}{F} \ln\left(\frac{[H_e^+]}{[H_i^+]}\right) \quad (15)$$

$$\Delta p = \Delta pH \frac{1}{1-u} \quad (16)$$

$$\Delta\Psi = \Delta p - \Delta pH \quad (17)$$

where $u = \Delta\Psi/\Delta p$ = constant.

The following expression for the buffering coefficient for internal protons was used:

$$b_H = c_{buff}/c_0 \quad (18)$$

where $c_{buff} = 0.022$ M H$^+$ per pH unit (assuming 1 μl matrix volume per mg of protein) is the buffering capacity measured experimentally and $c_0 = (10^{-pH} - 10^{-pH-dpH})/dpH$ is the "natural" buffering capacity for a given pH (dpH is a small change in pH).

Concentrations of free and magnesium-bound

forms of the most important magnesium ligands (X) were calculated in the following way:

$$[X^n_{fs}] = \frac{[X^n_{ts}]}{1 + \frac{[Mg^{2+}_{fs}]}{K_{D_{Xs}}}} \quad (19)$$

$$[X^n_{ms}] = [X^n_{ts}] - [X^n_{fs}] \quad (20)$$

where $[X^n]$ is the concentration of the nth ligand, index "s" denotes "i" or "e" indexes and K_D stands for a dissociation constant. The values of dissociation constants for particular magnesium ligands are given in Table 1. The total magnesium concentration was calculated as follows:

$$[Mg^{2+}_{ts}] = \sum_n [X^n_{ms}] + [Mg^{2+}_{fy}] \quad (21)$$

During simulations the free magnesium concentration was recalculated at each step, using 10 iterations:

$$[Mg^{2+}_{fs}] = [Mg^{2+}_{ts}] \Big/ \left(1 + \sum_n \left\{[X^n_{ts}]/\left([Mg^{2+}_{fs}] + K_{Dny}\right)\right\}\right) \quad (22)$$

When constant concentrations of free internal and external magnesium, both equal to 380 μM, were used, the properties of the model and the results of simulations were very similar.

The concentration of monovalent inorganic phosphate was calculated from the following expression:

$$[P_{i_{fs}}] = [P_{i_{ts}}]/(1 + q_s) \quad (23)$$

where

$$q_s = 10^{(pH_s - pK_a)}$$

and $pK_a = 6.8$.

The redox potentials of cytochromes c and a_3 were calculated from the redox potential of NAD and from the proton-motive force:

$$E_{hNAD} = E_{mNAD} + \frac{RT}{2F} \ln\left(\frac{[NAD^+]}{[NADH]}\right) \quad (24)$$

$$E_{mcyt.c} = E_{mNAD} + \Delta p(8 - 2u)/2 \quad (25)$$

$$E_{mcyt.a3} = E_{myct.c} + \Delta p(2 - 2u)/2 \quad (26)$$

Table 1
Dissociation constants of most important magnesium ligands

Ligand	Dissociation constant (μM)	
	Cytosolic space	Mitochondrial space
ATP	24	17
ADP	347	282
P_i	1180	1176
Citrate	270	238
MBP (magnesium binding pool)	710	221

The reduction levels of both cytochromes were obtained as follows:

$$[c^{3+}]/[c^{2+}] = e^{\left(\frac{E_{hcyt.c} - E_{mcyt.c}}{RT/F}\right)} \quad (27)$$

$$[a^{3+}]/[a^{2+}] = e^{\left(\frac{E_{hcyt.a3} - E_{mcyt.a3}}{RT/F}\right)} \quad (28)$$

The following values of mid-point redox potentials were used: $E_{mNAD} = -320$ mV, $E_{mcyt.c} = 250$ mV and $E_{mcyt.a3} = 556$ mV (the last value reflects, in fact, the mid-point redox potential for the cyt.a_3–Cu_B centre of cytochrome oxidase).

Concentrations of reduced and oxidized forms of cytochrome c and a_3 were calculated from their overall concentrations, $[c_t] = 0.8$ μM and $[a_t] = 0.4$ μM, respectively (these concentrations were determined in suspension, assuming amount of mitochondria equal to 3 mg of protein per ml).

In the model for isolated mitochondria incubated with succinate, only two proton pumps were taken into account and ubiquinone appeared instead of NAD in the above equations. A mid-point redox potential for ubiquinon equal to 85 mV was used.

2.4. Initial conditions

The initial (starting) point for all simulations performed using the model for cells (hepatocytes) represented the normal, physiological state. In the version of the model describing isolated mitochondria this initial point corresponded to "physiological" state 3.5, intermediate between state 4 and state 3 (about 50% of the respiration rate in state 3). The values of variables and parameters in the initial state were either fixed or calculated. In these calculations the criterion of thermodynamic requirements (a proper

direction and displacement from equilibrium of particular reactions) was taken into account. The initial state represented, of course, a steady-state (no changes in concentrations and fluxes).

The simulations performed in the present paper consisted in transition to another steady-state caused by a change in one of the parameter values. When the new steady-state was reached, the values of chosen variables were recorded. These values (for example, values of fluxes and thermodynamic forces) obtained in different steady-states were plotted one against another. In this way, dependence of one variable on another variable could be obtained.

Two kinds of transitions were studied. In aerobiosis → anaerobiosis transition different oxygen concentrations were fixed. At the initial point (both in cells and mitochondria) this concentration was equal to 240 μM. To obtain subsequent steady-states, lower and lower oxygen concentrations were imposed in subsequent simulations. As oxygen concentration enters the rate expression of cytochrome oxidase, the flux through this enzyme decreased, which was followed by changes in the entire system of oxidative phosphorylation. Particularly, Δp decreased and the reduction level of cytochrome c increased in order to compensate the resultant decrease in the oxygen consumption and ATP synthesis fluxes.

In simulations concerning state 4 → state 3 transition in isolated mitochondria the rate constant of ATP utilization was changed. This procedure corresponded to addition of different amounts of hexokinase in the presence of glucose (a frequently used artificial ADP-regenerating system) in order to fix different levels of energy demand under experimental conditions. When the value of this constant (or, which is equivalent, concentration of hexokinase) was reduced to zero, state 4 was reached, with no ATP synthesis and oxygen consumption corresponding exclusively to proton leak. A 6-fold increase in the rate constant of ATP consumption, in relation to the initial point, caused transition to state 3 (further increase in the value of this constant caused essentially no increase in oxygen consumption). All the remaining intermediate states were obtained by more moderate decrease or increase in the rate constant (concentration) of hexokinase.

In both versions of the model (for cells and for mitochondria) it was assumed that the "concentration" of mitochondrial proteins was equal to 3 mg per ml. A ratio of cell volume to mitochondrial volume (R_{cs}) equal to 10 was accepted. The ratio of suspension volume to cell volume (R_{sc}) was calculated as follows:

$$R_{sc} = \frac{[c_{tm}]}{[c_t]R_{cm}} \tag{29}$$

where $[c_{tm}] = 2700$ μM is the concentration of cytochrome c determined in matrix (calculated for matrix volume equal to 1 μl per mg protein) and $[c_t] = 0.8$ μM is the concentration of cytochrome c determined in suspension (for 3 mg of mitochondrial protein per ml). The obtained value of R_{sc} was equal to about 340. In the model for isolated mitochondria the ratio of external volume to matrix volume was equal to $R_{sc}R_{cm}$.

Table 2
Initial values of the respiration rate and components of the proton-motive force in the model for cells and for mitochondria

Variable	Cells	Mitochondria
Respiration rate (μM O_2 s^{-1})	1.0	1.7
Δp (mV)	182	175
ΔpH (mV)	27	25
$\Delta\Psi$ (mV)	155	150

The values of the respiration rate and components of Δp at the initial point for mitochondria and cells are shown in Table 2. The initial rates of particular reactions were calculated as follows: v_{c4} (oxygen consumption) was established (see Table 2); v_{LK} was calculated using Eq. 8; $v_{DH} = 2v_{c4}$; $v_{SN} = (n_c v_{c4} - v_{LK})/n_A$; $v_{UT} = v_{PI} = v_{EX} = v_{SN}$. A more detailed description of initial parameter and variable values is given in previous publications [10–13].

3. Test of the model

The dynamic model of oxidative phosphorylation used in this paper has been tested for a broad range of conditions, both in isolated mitochondria [10,11,13] and intact hepatocytes [10–12,14]. To increase the reliability of the theoretical results obtained, especially concerning thermodynamic aspects of cytochrome oxidase working in the entire oxida-

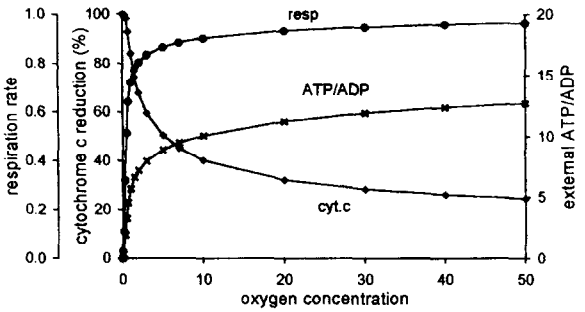

Fig. 1. Simulated dependencies of the respiration rate, cytochrome c reduction level and external ATP/ADP ratio on oxygen concentration. The respiration rate is expressed in arbitrary units (1 corresponds to the respiration rate at the saturated oxygen concentration: 240 μM).

tive phosphorylation system, it seems necessary to perform some more simulations using this model. They should concern cytochrome oxidase and thermodynamic properties of oxidative phosphorylation. The theoretical results obtained should be compared with experimental results.

The simulated dependencies of the respiration rate, cytochrome c reduction level and external ATP/ADP ratio on oxygen concentration in intact cells are shown in Fig. 1. They are very similar to the experimental results obtained by Wilson's group [15,16]. Since the mentioned parameters are strictly related (the ATP/ADP ratio through Δp) to the regulation of cytochrome oxidase, this agreement between simulations and experiments increases the reliability of the model.

Fig. 2 presents simulated flux–flow relationships for the oxidation and phosphorylation flux in isolated mitochondria. Changes in these fluxes, as well as in the phosphorylation potential (both in experiments and simulations), were obtained by an increase in ATP usage (addition of different amounts of hexokinase to mitochondria in state 4). The curves are near-linear, which mimics experimental results [1,17]. Such a linearity is broadly accepted in the frame of non-equilibrium thermodynamics applied to oxidative phosphorylation [1,3,17]. However, if we change the thermodynamic span through the system by decreasing the oxygen concentration (keeping concentrations of respiratory substrates as well as external ATP and ADP constant), we will obtain a non-linear relationship as presented in Fig. 3. It must be empha-

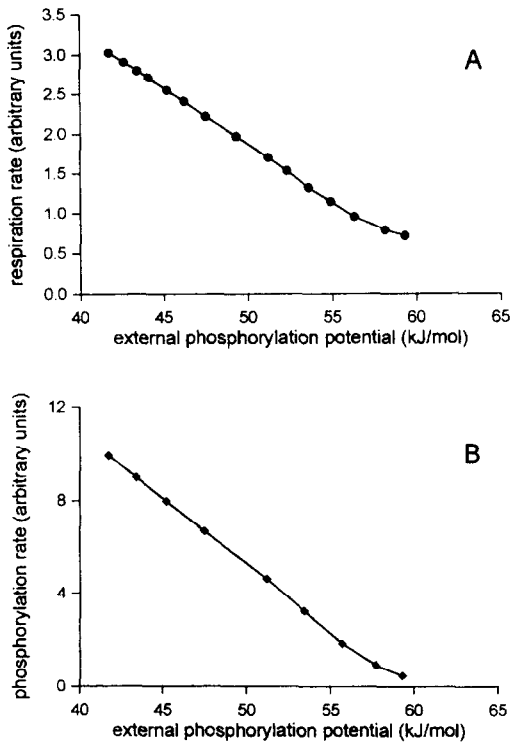

Fig. 2. Simulated flux–force relationships in isolated mitochondria for the entire oxidative phosphorylation system. (A) the oxidation flux plotted against the external phosphorylation potential; (B) the phosphorylation flux plotted against the external phosphorylation potential.

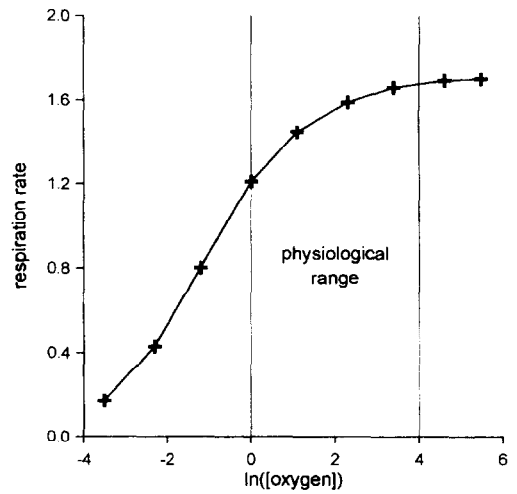

Fig. 3. A simulated dependence of the oxidation flux on the oxidation potential when this potential is changed by decrease in oxygen concentration.

sized that the latter property does not depend on the validity of the model. It is a simple result of an apparent Michaelis–Menten kinetic dependence of cytochrome oxidase-catalyzed reaction rate on oxygen concentration. The conclusion is that the flux–force relationship depends on the way in which the thermodynamic span through the system is changed.

Simulated titration curves of different enzymes and processes of oxidative phosphorylation by specific inhibitors (data not shown) are also very similar to those obtained experimentally [18,19].

4. Results

The total thermodynamic force X_{tot} corresponding to the reaction catalyzed by cytochrome oxidase is equal to

$$X_{tot} = X_H + X_c + X_O \tag{30}$$

where $X_H = -(2+2u)\Delta p$ indicates the proton-motive force multiplied by amount of protons (and charges) transported per two passing electrons ($u = \Delta\Psi/\Delta p$), $X_c = -2\Delta E_{h_{cyt.c}}$ indicates the redox potential of cytochrome c and $X_O = 2\Delta E_{h_{O_2}}$ indicates the redox potential of the O_2/H_2O pair. Concentration of water equal to 55 M as well as mid-point potentials of cytochrome c ($\Delta E_{m_{cytc}}$) and the O_2/H_2O pair ($\Delta E_{m_{O_2}}$) equal to 250 and 820 mV, respectively, were used in calculations. The thermodynamic potentials were calculated as follows:

$$\Delta E_{h_{cyt.c}} = \Delta E_{m_{cyt.c}} + \frac{RT}{F}\ln\left(\frac{[c^{3+}]}{[c^{2+}]}\right) \tag{31}$$

$$\Delta E_{h_{O_2}} = \Delta E_{m_{O_2}} + \frac{RT}{4F}\ln\left(\frac{[O_2]}{[H_2O]^2}\right) \tag{32}$$

$$\Delta p = \Delta\Psi + \Delta pH = \frac{1}{1-u}\Delta pH \tag{33}$$

$$\Delta pH = \frac{RT}{F}\ln\left(\frac{[H_e^+]}{[H_i^+]}\right) \tag{34}$$

Simulated changes in the total thermodynamic potential of the reaction catalyzed by cytochrome oxidase and in its component potentials during state 4 → state 3 transition (addition of increasing amounts of hexokinase to mitochondria in state 4 in the presence of glucose) are presented in Fig. 4. The overall thermodynamic span of cytochrome oxidase increases with the respiration rate. It can be seen that this is mainly a result of the increase in X_H (decrease in Δp). Since the oxygen concentration is kept constant, X_O does not change. X_c plays only a minor role in changes in X_{tot} as the reduction level of cytochrome c ($[cyt.c^{2+}]/[cyt.c^{3+}]$) varies very little. This suggests that the proton-motive force is the main factor regulating the rate of the reaction catalyzed by cytochrome oxidase during state 4 → state 3 transition.

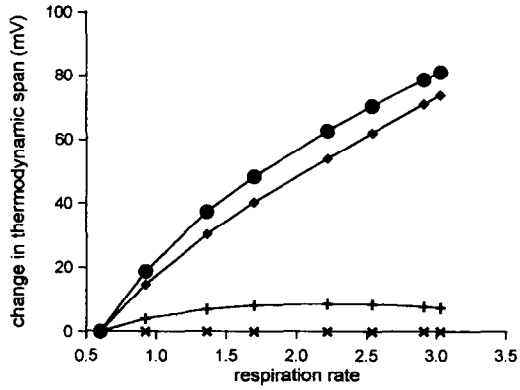

Fig. 4. Simulated changes of the total (X_{tot}, ●) and component (X_H, ◆; X_c, + and X_O, ×) thermodynamic potentials of the reaction catalyzed by cytochrome oxidase, plotted against the respiration rate during state 4 → state 3 transition. Values in state 4 are taken as reference values (0 mV change).

In Fig. 5 is shown a simulated dependence of the total thermodynamic span on the respiration rate

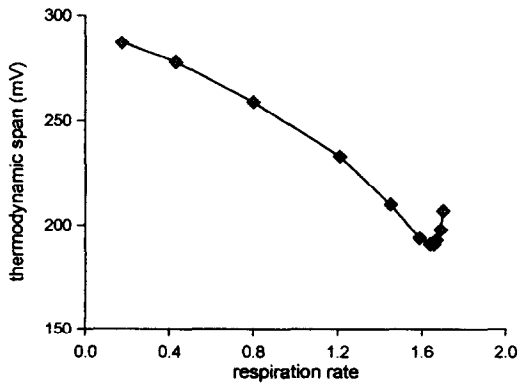

Fig. 5. A simulated dependence of the total thermodynamic span of the reaction catalyzed by cytochrome oxidase on the respiration rate during aerobiosis → anaerobiosis transition.

during aerobiosis → anaerobiosis transition (decreasing oxygen concentration). Despite the highest values of the respiration rate (corresponding to saturated oxygen concentrations), the relationship is inverse, i.e. the thermodynamic force increases when the respiration rate decreases.

The above changes in the total and component thermodynamic forces can be presented more clearly when plotted against the logarithm of oxygen concentration. This is shown in Fig. 6. The indicated physiological range of oxygen concentration is equal to about 1–100 μM [9]. It can be seen that the total thermodynamic force X_{tot}, changing proportionally to oxygen concentration at its higher values, becomes inversely dependent on oxygen concentration at oxygen concentrations below approximately 30 μM. Of course, X_O diminishes linearly with log([oxygen]). This is compensated by an increase in X_H and X_c. Below 30 μM, this compensation is so strong that the overall force X_{tot} begins to increase when oxygen concentration decreases.

The influence of the component thermodynamic potentials on the reaction rate of cytochrome oxidase depends not only on changes in these potentials, but also on elasticity coefficients [20] of the reaction to the considered potentials. The calculated values of these coefficients for X_H, X_c and X_O are equal to 11.2, 18.3 and 59.1, respectively. The calculations

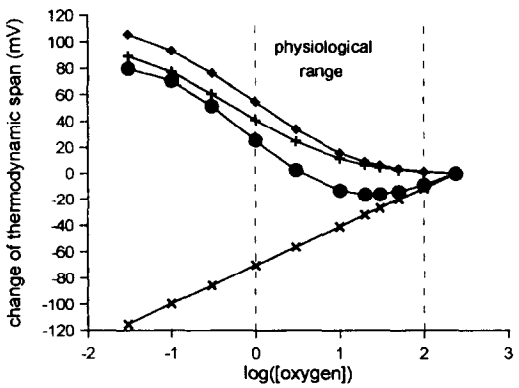

Fig. 6. Simulated changes of the total (X_{tot}, ●) and component (X_H, ◆; X_C, + and X_O, ×) thermodynamic potentials of the reaction catalyzed by cytochrome oxidase plotted against the logarithm of oxygen concentration during aerobiosis → anaerobiosis transitions. Values at saturated oxygen concentration (240 μM) are taken as reference values (0 mV change).

Table 3
Contributions of changes in the discussed thermodynamic potentials to changes in the respiration rate during state 4 → state 3 and aerobiosis → anaerobiosis transitions

Change in respiration rate	State 4 → state 3 transition	Aerobiosis → anaerobiosis transition
Δv_H	0.83	4.0
Δv_c	0.17	5.3
Δv_O	0	−10.3
Δv_{tot}	1	−1

Δv_H, Δv_c, and Δv_O indicate changes in the respiration rate caused by changes in X_H, X_c and X_O, respectively. Their values are standardized for the resultant change Δv_{tot}, being the sum of these changes, equal to 1 or −1.

were made for the "physiological" state $3_{1/2}$ (about 50% of the respiration rate in state 3) and median physiological oxygen concentration in mammalian tissues (about 30 μM [9]). The contributions of the three distinguished thermodynamic potentials to changes in the respiration rate during both state 4 → state 3 transition and aerobiosis → anaerobiosis transition are presented in Table 3. The values are standardized for the resultant change in the respiration rate equal to 1 (or −1). These results show that a decrease in Δp is responsible for more than 80% of the increase in the respiration rate during state 4 → state 3 transition, while the contribution of the cytochrome c reduction level is less than 20%. During aerobiosis → anaerobiosis transition changes in X_H and X_c compensate over 90% of the decrease in the respiration rate caused by decreasing oxygen concentration (without this compensation the respiration rate would decrease by 10.3 instead of by 1, in arbitrary units). Their action is quantitatively comparable. The reduction level of cytochrome c has an even slightly stronger influence than the proton-motive force, unlike during state 4 → state 3 transition.

5. Discussion

Of course the main condition of reliability of the theoretical results obtained is validity of the model used for calculations. A reasonable criterion for this validity seems to be the number of different conditions and experiments the model has been tested for. This model simulated successfully the following pa-

rameters and properties of oxidative phosphorylation:

- changes in different parameter values (respiration rate, Δp, reduction level of cytochrome c, internal and external ATP/ADP ratio and others) during state 4 → state 3 transition in isolated mitochondria [13],
- time courses of these parameters after addition of a small amount of ADP to mitochondria in state 4 (state 4 → state 3 → state 4 transition) [13],
- flux control coefficients for different components of oxidative phosphorylation with respect to the respiration flux at different respiration rates between state 4 and state 3 [13], obtained in the frame of metabolic control analysis (MCA) [21],
- flux control coefficients for the oxidation, phosphorylation and proton leak subsystems over the oxidation (respiration), phosphorylation and proton leak fluxes at different respiration rates between state 4 and state 3 [13], obtained in the frame of the "top-down approach" to MCA [22],
- time courses of different parameter values during consumption of oxygen by suspension of cells (or mitochondria) in a closed chamber (aerobiosis → anaerobiosis transition) [10,12],
- kinetic responses of oxidation, phosphorylation and proton leak subsystems to Δp in hepatocytes incubated with different respiratory substrates [12],
- values of the respiration rate, cytochrome c reduction level and external ATP/ADP ratio at different oxygen concentrations (this paper),
- linear flux-force relationships, similar to those obtained for oxidative phosphorylation in the frame of non-equilibrium thermodynamics (NET) (this paper),
- inhibitor titration curves for cytochrome oxidase, ATP/ADP carrier and other components of oxidative phosphorylation, obtained experimentally in the frame of MCA (this paper, not shown).

The agreement between simulations and experiments was at least semi-quantitative and in many cases very good. Therefore, it can be assumed that the model is able to produce, at least qualitatively (and probably semi-quantitatively), correct predictions in the range of conditions it has been tested for.

Additionally, some theoretical results presented in this paper do not depend on the validity of the model. Changes of thermodynamic potentials (X_H, X_c and X_O) during aerobiosis → anaerobiosis transition can be extracted from experimental data mimicked in Fig. 1 (see, for example, Fig. 2 in [15]). In this case, the model only helps to obtain the desired parameter values easily and conveniently.

In the present study the dependence of cytochrome oxidase on whole Δp is considered, although influence of its components, namely ΔpH and $\Delta\Psi$, has been shown to be different [8]. However, it was demonstrated, at least under steady state conditions, that a linear dependence between ΔpH and $\Delta\Psi$ takes place [23].

The obtained agreement between simulations and experiments suggests that no additional mechanisms (for example allosteric regulation proposed in [6]) are necessary to explain the observed kinetic properties of cytochrome oxidase.

The first conclusion drawn from the simulations performed is that the flux–force relationship can depend on the way in which the relevant thermodynamic force is changed. For both cytochrome oxidase and the whole oxidative phosphorylation system this relationship is near-linear for state 4 → state 3 transition (or for varying respiratory substrate concentrations [1]) and non-linear for aerobiosis → anaerobiosis transition. Therefore, the linear approximation used in the frame of NET seems not to be universal.

Furthermore, the flux–force relationship can be inverse in some situations, which contradicts intuitive expectations. However, such a possibility can be explained in a simple way. Let us consider the following reaction:

$$A + B \xrightarrow{v} C$$

where A and B are converted into C at a rate v. The thermodynamic span of this reaction is proportional to log([A][B]/[C]). Let us assume that elasticities of v to A and B are equal to 1 and 5, respectively. Now, if [A] increases by 4% and [B] decreases by 2% ([C] is kept constant), the rate v will decrease by 6% while the [A][B]/[C] ratio (and the thermodynamic span) will increase. It can happen because elasticity of v to B is essentially higher then the elasticity of v to A. A similar situation occurs for cytochrome oxidase: the elasticity of the respiration

rate to X_O is much greater than its elasticity to X_H or X_c.

The increase in the total thermodynamic span of the reaction catalyzed by cytochrome oxidase when oxygen concentration decreases can be interpreted as a "thermodynamic cost" of kinetic regulation. The purpose of this regulation is to keep the respiration rate as constant as possible when oxygen pressure decreases. This leads, because of kinetic properties of cytochrome oxidase, to "overcompensation" of the decrease in X_O by the increase in X_H and X_c. The theoretical results obtained suggest that, in the case of decrease in oxygen concentration, it is more important for the cell to optimize the flux through cytochrome oxidase rather than the thermodynamic force of the reaction catalyzed by this enzyme. Thermodynamic efficiency is here sacrificed in order to maintain oxygen consumption and ATP synthesis unchanged.

However, it is important for the cell to maintain not only a high rate of ATP production, but also a high concentration of this compound or, rather, a high value of the external phosphorylation potential. When oxygen concentration decreases below 30 μM, cytochrome oxidase becomes more and more displaced from equilibrium, partially because Δp decreases significantly. Since the ATP synthase is supposed to work near equilibrium, the value of the internal phosphorylation potential should follow changes in the proton-motive force. The external phosphorylation potential is related to the internal phosphorylation potential mainly through the ATP/ADP carrier. As it was shown in previous theoretical studies [4], this carrier has a high positive value of the thermodynamic response coefficient during aerobiosis → anaerobiosis transition. Therefore, its displacement from equilibrium diminishes very quickly when oxygen concentration falls down. As the result, the external phosphorylation potential decreases much slower than the internal one. Thus, the ATP/ADP carrier acts as a "thermodynamic buffer", keeping the external phosphorylation potential as constant as possible, when oxygen concentration, Δp and the internal phosphorylation potential decrease. Generally, the concomitant action of cytochrome oxidase and the ATP/ADP carrier causes that both the rate of ATP synthesis and the external phosphorylation potential remain relatively high even at low (a few μM) oxygen concentrations. Therefore, despite the fact that the thermodynamic efficiency of cytochrome oxidase decreases significantly when oxygen concentration decreases, the efficiency of the whole system remains much more constant due to the "thermodynamic buffering" by the ATP/ADP carrier and some other steps [4].

The last suggested conclusion is that the regulation of cytochrome oxidase is different under the same conditions, when different changes are introduced into the oxidative phosphorylation system. Cytochrome oxidase is activated mainly by increase in X_H in response to increased energy demand (state 4 → state 3 transition). On the other hand, decrease of the rate of the reaction catalyzed by this enzyme at lower oxygen concentrations is compensated by increase in both X_c and X_H to a comparable extent. Therefore Δp seems to be an universal regulatory factor of cytochrome oxidase, while the reduction level of cytochrome c probably plays an important role mainly in compensation of decrease in oxygen concentration.

6. Abbreviations

X_{tot}	total thermodynamic span of the reaction catalyzed by cytochrome oxidase
X_H	$= -(2 + 2u)\Delta p$
X_c	$= -2\Delta E_{cyt.c}$
X_O	$= 2\Delta E_{h_{O_2}}$
u	$= \Delta\Psi/\Delta p$ = constant
Δp	proton-motive force
$\Delta E_{hcyt.c}$	redox potential of cytochrome c
$\Delta E_{h_{O_2}}$	redox potential of the O_2/H_2O pair
e	external
i	internal
s	external or internal
t	total
f	free
m	magnesium complex
j	monovalent

Acknowledgements

This work was supported by a KBN grant.

References

[1] H. Rottenberg, Biochim. Biophys. Acta, 549 (1979) 225–253.
[2] H. Rottenberg, Biophys. J., 13 (1973) 503–511.
[3] H.V. Westerhoff and K. van Dam, Thermodynamics and Control of Free-Energy Transduction, Elsevier, Amsterdam, 1987.
[4] B. Korzeniewski and W. Froncisz, in S. Schuster, M. Rigoulet, R. Ouabi and J.-P. Mazat (Eds.), Modern Trends in BioThermoKinetics, Plenum Press, New York, 1993.
[5] J.G. Reich and E.E. Selkov, Energy Metabolism of The Cell, A Theoretical Treatise, Academic Press, London, 1982.
[6] B. Kadenbach, J. Bioenerg. Biomembr., 18 (1986) 39–54.
[7] N.L. Greenbaum and D.F. Wilson, Biochim. Biophys. Acta, 1058 (1991) 113–120.
[8] S. Papa, in T.E. King, H.S. Mason and M. Morrison (Eds.), Oxidases and Related Redox Systems, Alan R. Liss, New York, 1988.
[9] C.G. Brown, Biochem. J., 284 (1992) 1–13.
[10] B. Korzeniewski and W. Froncisz, Biochim. Biophys. Acta, 1060 (1991) 210–223.
[11] B. Korzeniewski and W. Froncisz, Biochim. Biophys. Acta, 1102 (1992) 67–75.
[12] B. Korzeniewski, Biophys. Chem., submitted for publicaton.
[13] B. Korzeniewski, Biophys. Chem., submitted for publication.
[14] B. Korzeniewski, M.-E. Harper and Brand, Biochim. Biophys. Acta, 1229 (1995) 315–322.
[15] D.F. Wilson, M. Erecińska, C. Drown and I.A. Silver, Arch. Biochem. Biophys., 195 (1979) 485–493.
[16] T. Kashiwagura, D.F. Wilson and M. Erecińska, J. Cell Physiol., 120 (1984) 13–18.
[17] J.W. Stucki, Eur. J. Biochem., 109 (1980) 269–283.
[18] F.N. Gellerich, R. Bohnensack and W. Kunz, Biochim. Biophys. Acta, 722 (1983) 381–391.
[19] T. Letellier, R. Heinrich, M. Malgat and J.-P. Mazat, Biochem. J., 302 (1994) 171–174.
[20] H. Kacser and J.W. Porteous, Trends Biochem. Sci., 12 (1987) 5–14.
[21] A.K. Groen, R.J.A. Wanders, H.V. Westerhoff, R. van der Meer and J.M. Tager, J. Biol. Chem., 267 (1982) 2754–2757.
[22] R.P. Hafner, G.C. Brown and M.D. Brand, Eur. J. Biochem., 188 (1990) 313–319.
[23] J. Duszyński, K. Bogucka and L. Wojtczak, Biochim. Biophys. Acta, 767 (1984) 540–547.